

# **WIRE ARC ADDITIVE MANUFACTURING OF CP-TITANIUM BIO-MEDICAL ALLOY**

**M.Tech Thesis**

By  
**ABHINAV KATIYAR**  
(2002103001)



**DEPARTMENT OF MECHANICAL ENGINEERING  
INDIAN INSTITUTE OF TECHNOLOGY  
INDORE**

**MAY 2022**





# INDIAN INSTITUTE OF TECHNOLOGY INDORE

## CANDIDATE'S DECLARATION

I hereby certify that the work which is being presented in the thesis entitled **WIRE ARC ADDITIVE MANUFACTURING OF BIO-MEDICAL ALLOY** in the partial fulfillment of the requirements for the award of the degree of **MASTER OF TECHNOLOGY** and submitted in the **DISCIPLINE OF MECHANICAL ENGINEERING, Indian Institute of Technology Indore**, is an authentic record of my own work carried out during the time period from August 2020 to May 2022 under the supervision of **Dr. Dan Sathiaraj, Associate Professor, Department of Mechanical Engineering, Indian Institute of Technology** and **Dr. I.A. Palani, Professor, Department of Mechanical Engineering, Indian Institute of Technology**.

The matter presented in this thesis has not been submitted by me for the award of any other degree of this or any other institute.

Abhinav  
01/06/2022

Signature of the student with date  
(ABHINAV KATIYAR)

-----  
This is to certify that the above statement made by the candidate is correct to the best of my/our knowledge.

  
(Dr. Dan Sathiaraj)  
31/05/22

for   
(Dr. I.A. Palani)  
31/05/22

-----  
ABHINAV KATIYAR has successfully given his/her M.Tech. Oral Examination held on 23 May 2022.

  
Signature(s) of Supervisor(s) of M.Tech. thesis  
Date:

  
Signature of PSPC Member  
(Dr, Sumanta Samal)  
Date: 01/06/2022

  
Convener, DPGC  
Date: 01.06.2022

  
Signature of PSPC Member  
(Dr. Girish Chandra Verma)  
Date: 01.06.2022



## ACKNOWLEDGEMENTS

To begin, I'd like to express my gratitude to my project supervisor, **Dr Dan Sathiaraj**, for providing me with this wonderful opportunity and for his continued support as I work under their supervision and try to learn more about equal channel angular pressing of medium entropy alloys. The constructive discussions, suggestions, and regular reviews act as a means of inspiration for conducting a thorough analysis of the stated problem statement. My sincerest appreciation to PSPC members **Dr Sumanta Samal** and **Dr Girish Chand Verma** for taking the time to evaluate my work and using their extensive knowledge to provide constructive feedback to attain the desired results. I would also like to extend my thank to **Dr. Avinash Sonawane** for letting me use the facilities of his laboratories for my project work.

I would also like to thank all of the members of the **Mechatronics and Meteorology lab** and the **Gear lab** for their unwavering support in carrying out my project. I would like to show my thankfulness to research scholar **Miss Poonam Deshmukh**, **Mr. Anshu Sahu**, **Miss. Ananyaashree Behera** and the entire **IITI Central workshop staff** for their assistance and insights into the experimental elements and potential problems encountered when conducting deposition and characterization of CP-Ti.

Indeed, I will not be able to conclude my thoughts without expressing my heartfelt thanks and appreciation to all of my colleagues who have faced equally difficult challenges and yet have remained steady and persistent in achieving their goals and motivating me to keep working hard. Through this, I'd like to express my gratitude to everyone who has aided me in my research work, both directly and indirectly, at different stages of the project.

With sincerest regards,

Abhinav Katiyar



*Dedicated*  
*to*  
*My beloved*  
*Parents, Brother*  
*and Bhabhi*

## Abstract

Metal additive manufacturing system is a process of fabricating metallic parts by direct fusion in a layer upon layer manner, either using metallic powder or wire as feedstock. Microstructure, mechanical properties, and biocompatibility of WAAM-built samples is investigated. The track deposition is performed to know the optimum process parameters and wall structure is fabricated at these known process parameters. Further, characterization is performed to study the microstructure variations with post processing, such as heat treatment and laser shock peening. The as-built samples exhibited dominance of  $\alpha$ -phase as revealed from XRD peaks. Heat treatment at 900°C is carried out in vacuum to achieve phase transformation from  $\alpha \rightarrow \beta$  phase. The increase in fraction of  $\beta$ -phase after heat treatment is confirmed by XRD phase analysis and microscopic images as well. The Laser Shock Peening (LSP) effect is observed up to a depth of 43.4476 $\mu\text{m}$  along cross-section. The LSP further improved the surface micro-hardness of heat treated samples. The anti-bacterial biocompatibility test has signified that the LSP treated sample gave better antibacterial effect to the sample surface.

# TABLE OF CONTENT

## Contents

<b>Chapter1 .....</b>	<b>1</b>
<b>Introduction.....</b>	<b>1</b>
<b>1.1 Additive Manufacturing .....</b>	<b>1</b>
<i>1.1.1 Classification of AM Processes .....</i>	<i>2</i>
<i>1.1.1.2 Binder Jetting .....</i>	<i>2</i>
<i>1.1.1.3 Direct Energy Deposition .....</i>	<i>3</i>
<i>1.1.1.4 Sheet Lamination .....</i>	<i>3</i>
<b>1.2 Wire Arc Additive Manufacturing (WAAM) .....</b>	<b>3</b>
<i>1.2.1 MIG-Based WAAM.....</i>	<i>3</i>
<i>1.2.2 TIG-Based WAAM.....</i>	<i>4</i>
<b>1.3 Heat Treatment .....</b>	<b>4</b>
<i>1.3.2 Normalizing.....</i>	<i>5</i>
<i>1.3.3 Quenching.....</i>	<i>5</i>
<i>1.3.4 Tempering .....</i>	<i>6</i>
<b>1.4 Laser shock peening.....</b>	<b>6</b>
<b>1.5 Biocompatibility .....</b>	<b>6</b>
<b>1.8 In-Vitro Assessment.....</b>	<b>9</b>
<b>Chapter 2 .....</b>	<b>11</b>
<b>Literature Review .....</b>	<b>11</b>
<i>Literature Gap .....</i>	<i>16</i>
<b>Objectives .....</b>	<b>17</b>
<b>Chapter 3 .....</b>	<b>19</b>
<b>Experimental Program.....</b>	<b>19</b>
<b>3.1 Design of experiments.....</b>	<b>19</b>
<b>3.2 WAAM of CP-Ti .....</b>	<b>20</b>
<b>3.3 Metallographic Sample preparation and Characterization..</b>	<b>21</b>
3.3.1 Wire EDM(W-EDM) .....	21
3.3.2 Metallography Steps used for sample preparation.....	21
3.3.3 Etching .....	22
<b>3.4 Heat Treatment of cut samples.....</b>	<b>22</b>
<b>3.5 Laser Shock Peening.....</b>	<b>23</b>

3.6 Microhardness testing .....	24
3.7 Biocompatibility Testing .....	24
<b>Chapter 4 .....</b>	<b>29</b>
<b>Results &amp; Discussion.....</b>	<b>29</b>
4.1 Process Parameter Optimization.....	29
4.2 Surface Porosity Measurement.....	30
4.3 Microstructure Study .....	31
4.4 Elemental Mapping Study.....	33
4.5 Phase Analysis .....	34
4.6 Micro Hardness Analysis .....	36
4.7 Bio-compatibility Analysis .....	37
<b>Chapter 5 .....</b>	<b>39</b>
<b>Conclusions and Future Scope.....</b>	<b>39</b>
5.1 Conclusions.....	39
5.2 Future Scope.....	40
<b>References.....</b>	<b>43</b>

## LIST OF FIGURES

Figure 1.1 shows the Classification Metal Additive manufacturing

Figure 1.2 Heat Treatment processes deployed commonly after AM

Figure 3.1 Setup for Wire Arc Additive Manufacturing

Figure 3.2 Heat Treatment setup used (a) Vacuum Glass tube

(b) Muffle Furnace

Figure 3.3 Laser Shock Peening Setup

Figure 3.4 Steps utilized during Anti-Bacterial Testing

Figure 3.5 Petri dish prepared for Anti-Bacterial Testing

Figure 4.3 Track deposition for parameter optimization

Figure 4.4 Track Characterization

Figure 4.5 Surface Porosity Measurement

Figure 4.6 Optical Image of CP-Ti as-built in deposition direction

Figure 4. 5 Optical Image of CP-Ti after Heat Treatment (a)for 30 minutes;(b) for 90 minutes

Figure 4.6 Optical Image of CP-Ti after Heat Treatment (a)for 30 minutes;(b) for 90 minutes

Figure 4.7 EDX of CP-Ti along (a) Deposition Direction; (b) Build Direction

Figure 4.8 XRD peaks of as-built CP-Ti along (a) Deposition Direction; (b) Build Direction

Figure 4.9 XRD peaks of Heat Treated CP-Ti (a) for 30 minutes; (b) for 90 minutes

Figure 4.10 Vicker's Micro Hardness variation at different conditions

Figure 4.11 Bacteria Colony Growth in Petri Dish

## LIST OF TABLES

Table 1.1 Mechanical properties of CP-Ti

Table 1 .2 Chemical Properties of CP-Ti

Table3.1 Taguchi's L9 Orthogonal Array

Table 3.2 Experimental parameters

Table 3.3 Optical Density Measurement

Table 4.1 Length matrix to determine average affected depth after  
LSP

Table 4.2 Average Micro Hardness Values





# Chapter1

## Introduction

The most crucial industrial revolution is the revolution through manufacturing. Manufacturing is the process of converting raw materials or parts into complete finished products by the investment of human labor, tools, and raw material. Historically, the Industrial revolution was born in England; rapid growth of industrialization was fueled by the generation of wealth, which also gave bloom to the colonization.

The conventional manufacturing process can be classified into major groups like Forging, Casting, Welding, Machining, and Metallurgy.

Industrialization is an important factor in the economic development of a country, and with the race among nations for the industrialization, there is an exponential growth towards industrialization 4.0. The digital revolution fundamentally affects the lifestyle of individuals and provides more opportunities, and offers a sustainable lifestyle. Industrial 4.0 has also affected Manufacturing processes which gave nudge to Additive Manufacturing as an advanced green manufacturing technology.[1]

### 1.1 Additive Manufacturing

Additive manufacturing often referred to as 3D printing, is an innovative method for the manufacturing of light weight, high strength, and complex geometry products which is not possible to be manufactured using conventional manufacturing processes. Additive manufacturing takes up data from CAD software or 3D object scanners which is used to create data file of .stl (STereo Lithography) format, which is often referred to as "Standard Triangle Language" and "Standard Tessellation Language." In this file the object is sliced into ultra-thin layers. The information mentioned in STL is used to guide nozzle or print head mounted on the guidepost (CNC axis stage) to deposit the raw material in the form of powder or wire layer by layer to form the three-dimensional product. The nozzle or print head can be

mounted on the vertical axis of the CNC stage or the complete work-bench on which the substrate is kept can have feed in all three axes.[2]

### ***1.1.1 Classification of AM Processes***

Metal Additive manufacturing depending upon the type and the process by which raw material is supplied is classified as:

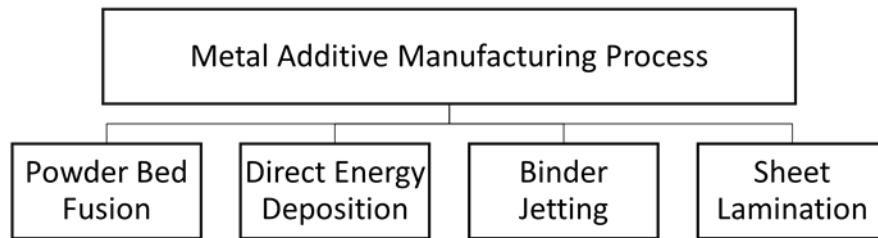


**Figure 1.1 shows the Classification Metal Additive manufacturing**

### **Powder Bed Fusion**

PBF technology uses raw material in the form of powder particles at micron level size. The powder particles are fused using a laser or electron beam as a heating source to build up a complex array of three-dimensional products. The high precision and remarkable freedom of design are provided to the manufacturer in this technique. SLM process includes various processes like Direct metal laser sintering (DMLS), Electron beam melting (EBM), Selective laser melting (SLM), and Selective laser sintering (SLS). [3]

#### ***1.1.1.2 Binder Jetting***

Binder jetting technology setup consists of two beds: powder and build bed. During processing the powder from the powder bed is brought into the build bed with the help of a roller followed by supplying a liquid binder from the print head and selectively placing it on the powder region to solidify the powder, and repeating the process until a fully consolidated component is formed, the part produced is further sintered in a furnace for debinding. The typically used binder for

metals is aqueous-based. Since no heat is applied in making the green part, lesser residual stresses are present in the fabricated part.[3]

### ***1.1.1.3 Direct Energy Deposition***

DED uses a laser, electron beam, plasma, or arc as energy sources to melt material either in the powder form fed through a nozzle or a separate wire feedstock to form a 3D object. During this process, a molten melt pool is created. Therefore, typically, DED is performed in a hermetically sealed chamber filled with inert gas (mostly, Argon) or vacuum to prevent oxidation. [4] DED includes laser directed energy deposition (LDED), Electron beam direct energy deposition (EB-DED), Arc assisted energy deposition also referred to as wire arc additive manufacturing (WAAM). [5]

### ***1.1.1.4 Sheet Lamination***

Sheet Lamination (SL), commonly known as laminated item manufacture, is a type of laminated object manufacturing. This process uses thin metallic sheets as raw material which is precisely cut and stacked together to form a 3D desired object. A localized energy source, mostly ultrasonic is used to bind the stack of sheet. This technique is also referred to as Ultrasonic additive manufacturing (UAM) since an ultrasonic energy source is used.[3]

## **1.2 Wire Arc Additive Manufacturing (WAAM)**

WAAM is a type of direct energy deposition method which uses arc as the energy source to melt the raw material in the form of wire. The automation torch is generally mounted on the vertical axis of the CNC stage, and other two axes guide the work-piece, here, substrate. WAAM system is based on the basic principle of welding, therefore, depending upon the principle WAAM can be sub-categorized into MIG-based and TIG-based.

### ***1.2.1 MIG-Based WAAM***

In MIG DC source of reverse polarity is used that means the electrode is kept as positive and the substrate is kept negative. The reverse

polarity is used as during electric transfer between the anode and cathode with a gap present 70% of the heat is generated at the anode. Since during MIG we need to melt wire. Therefore, we connect a wire to the positive terminal. By using this principle of MIG we deposit bead on the substrate with a continuous, uninterrupted motion, and further deposition is done on the previous bead to form a wall structure. [6]

### ***1.2.2 TIG-Based WAAM***

In TIG AC or DC power source of forward polarity is used, and the substrate is kept positive in case of DC source is used so that a larger amount of heat is generated on the substrate, the electrode used is of Tungsten and is of non-consumable type. The type of power source used depends upon the material for which the process is being used. The wire is fed externally to the arc produced between the substrate and the tungsten electrode, and the bead is deposited on the substrate.

## **1.3 Heat Treatment**

It is the process of heating metal below its melting point temperature or to the recrystallization temperature and further controlled cooling of the heated metal to get the desired properties. Heat Treatment is done to improve surface properties like hardness and bulk properties like malleability, ductility, toughness, and resilience. Heat Treatment is also helpful in varying the property of the metal, like elasticity and strength of the metals. The rate of cooling employed to the metal after heating it to the recrystallization temperature has different phenomena like stress relieving, hardening, change in grain orientation, and grain size.[7] Various types of heat treatment processes depending on the rate of heating and cooling employed are as shown in Figure1.2.

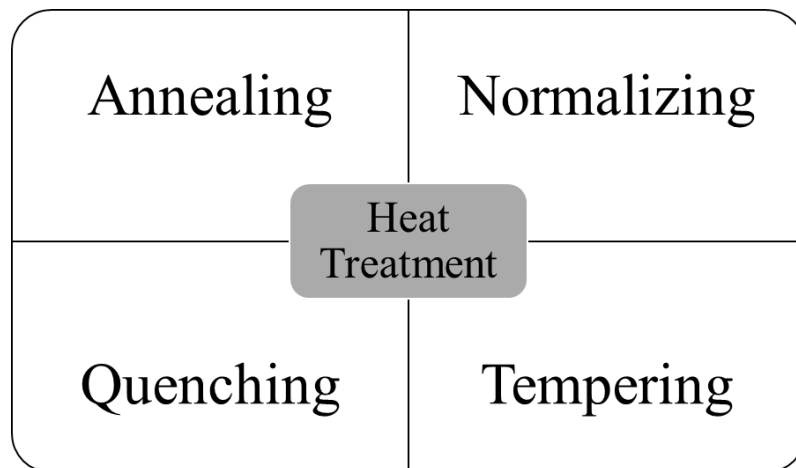


**Figure 1.2 Heat Treatment processes deployed commonly after AM**

### **1.3.1 Annealing**

During annealing, the material is heated to a predetermined temperature and then held at that temperature for a certain amount of time, and then cooled at a gradual rate by keeping the material in the furnace during cooling. Annealing accomplishes relieving internal stresses, improvement or restoration of ductility and toughness, refinement of grain size. [8]

### **1.3.2 Normalizing**

Normalizing is the process in which the material is heated to a predetermined temperature and then held at that temperature for a certain duration, and then cooled to room temperature in air. The process of normalizing is mainly employed for grain refinement. Thus, finer grain size is obtained using this process in comparison to annealing.[8]

### **1.3.3 Quenching**

During this process, the material is heated to a predetermined, holding at that temperature and then water or brine solution is used as a cooling medium for rapid cooling rate. After this process, high hardness and fine grain size are obtained. In some instances, the phase transformation is a reason for the high hardness value. [8]

### ***1.3.4 Tempering***

In the process of tempering, the material is heated to an elevated temperature. Still, not too high temperature is kept at elevated temperature for a certain amount of time and then cooled slowly. The motive behind tempering is basically to reduce hardness and relieve internal stress. This process mostly follows above-mentioned heat treatment processes.[8]

### **1.4 Laser shock peening**

Rapid irradiation of the surface with a high-power laser with a short pulse time is when applied, generates a shock wave and results in alteration of microstructure. The plasma induced shock wave during the process causes plastic deformation at the surface and induces compressive residual stresses.[9] Selection of a suitable laser with a high repetition rate and wavelength are some of the most important parameters for the success of the LSP process. In recent scenarios, for the process of LSP is carried out using laser beams produced by a Q-switched laser system based on yttrium aluminum garnet (YAG) crystal lasing rod, the operating range of the mentioned laser is near-infrared i.e. 1064nm and pulse duration in the range of 10-100 ns. [10]

During the LSP process, the intense laser beam is incident upon the laser surface for a short period of time, approximately 30 ns and the heated zone temperature reaches around 10,000°C. This heated zone due to high temperature and ionization, transforms into plasma and the plasma produced absorbs the energy from laser. The plasma generates the pressure by absorbing the energy from the laser and transmitting it to the material as a shock wave. Depending upon the interaction of laser to the material surface LSP is categorized as Direct Ablation type and Confined Ablation type. [10]

### **1.5 Biocompatibility**

Biocompatibility continues to be described as per ISO 10993-1: 2018 standard, “The ability of a material to perform with an appropriate host

response in a specific application.” (*Williams 1987*) The practical approach used to determine whether a particular device or implant is biocompatible depends on its biological response, and it does not introduce any unreasonable harm to users.[11] Tools used for Biocompatibility of devices are analytical chemistry, in vitro tests, and animal models. Factors on which biocompatibility depends upon [12]

- the chemical and physical nature of its component materials
- the types of patient tissue that will be exposed to the device
- the duration of that exposure

Some of the recommended biocompatibility tests for the testing of biomedical implants are:

- **Cytotoxicity Test (Tissue Culture)**

This test is a useful approach for screening materials prior to in-vitro testing.

- **Sensitization Assays**

This study assists in to establish whether a substance includes compounds that have adverse local or systemic effects after repeated or extended contact.

- **Implantation Tests**

This study quantifies the local irritation potential of materials by employing at locations such as skin or mucous membranes, generally in an animal model.

## **1.6 Biomaterials**

The Clemson University Advisory Board for biomaterials has formally defined biomaterial as “A systemically and pharmacologically inert substance designed for implantation within or incorporation with living systems.”[13] Because of the biomaterials' efficient and dependable properties, they are used inside a physiological medium. Metallic implant material possesses substantial clinical value. The essential properties that

a biomaterial must have to perform adequately as an implant in a biological system are- nontoxic, biocompatibility, and absence of foreign body reactions. Metals like Stainless steel (316L), titanium and alloys (CP-Ti, Ti6Al4V), cobalt-chromium alloys (Co-Cr), aluminium alloys, zirconium niobium, and tungsten heavy alloys were few of the materials available for biomedical application. The major factors on which the material to be used depends upon the biological environment and function to be performed. 316L stainless steel is mostly used for implants used for cardiovascular, otorhinology, and many more. For high wear resistance, such as artificial joints, CoCrMo alloys are used.[14]

## 1.7 CP-Ti

Titanium (Ti) and its alloys have the best biocompatibility among the major metallic biomaterials. [15] Ti alloys owing to their high specific ratio (i.e., tensile strength divided by density), allows versatile design during the dental application, and good corrosion resistance is used for biomedical application. Titanium and its alloys composed of three structures forms being  $\alpha$ ,  $\beta$ , and  $\alpha+\beta$ . Commercially pure titanium (CP-Ti). Allotropically, commercially pure titanium (CP-Ti) changes from a hexagonal close pack (HCP) crystal structure to a body-centered cubic crystal structure (BCC) at 882.5°C. [16] However, CP-Ti's low surface hardness, low mechanical strength, and poor wear resistance constrain and limit its vast variety of applications.

**Table 5.1 Mechanical properties of CP-Ti[16]**

<b>Properties</b>	<b>Value</b>
<b>Tensile Strength</b>	275-410 MPa
<b>Elongation</b>	20%
<b>Modulus of Elasticity</b>	105 GPa

**Table 1 .2 Chemical Properties of CP-Ti [15]**

<b>Element</b>	<b>Fe</b>	<b>O</b>	<b>C</b>	<b>N</b>	<b>H</b>	<b>Ti</b>
<b>Content(%)</b>	0.300	0.250	0.080	0.030	0.015	Balance

## **1.8 In-Vitro Assessment**

In vitro assessment is defined as, “A test setup that produces cells extracted from a living organism outside the body in controlled laboratory conditions.”[17] To ensure the life of living organisms, cells are harvested from a living creature and stored in appropriate environmental conditions that include all necessary organic and inorganic materials, water, temperature, and so forth. In-vitro testing is useful for studying the biological behavior of materials without causing serious harm to animals as in-vivo testing does. Since the In-Vitro study gives rapid results and can be done in a wide range of models, the duration for the testing is small. Additionally, the repeatability of tests within a short period of time makes it an ideal process. The In-Vitro assessment involves an initial selection of tissue cells. Further, testing for the potential to damage the selected tissue depending on the host environment. Also, the materials previously proven safe can be re-tested for chemical or surface modifications. The cell culture system in In-Vitro helps in assessing the toxicity of material for all the related cell arrays. Bacterial or fungi culture is also used to gauge the antimicrobial effect of the material to be tested. Germs cultivated in a certain environment are exposed to the material to be tested, and the number of microorganisms that survive is counted to evaluate potency.[14]



## Chapter 2

### Literature Review

This chapter gives insight into the methodology and technology available in Metal additive manufacturing (MAM) and post-processing techniques such as laser shock peening and heat treatment for biomedical applications. Biocompatibility testing and various methods used are also being highlighted in this chapter. AM is an advanced manufacturing technique that involves layer by layer addition with a CNC automation system. AM techniques and relative process parametric optimization play a major role during the experimental work. AM technique is governed by fusion and deposition, which in turn is influenced by speed, power, and feed rate. In this chapter, we get to know various techniques being used for the AM of biomedical alloys and the influence of post-processing on the material properties, and their effect on the application area.

**Bartłomiej Wysocki et al.**[18] proposed a metal 3D printing process based on SLM of titanium in a reactive atmosphere, i.e., in an Oxygen atmosphere which provides higher strength with no expense to ductility. In this work, based on sets of micro-samples cut from the whole volume, the anisotropy of the produced part was examined in different cross-sections. The defect free deposition without any partially melted powder, pores, and balling effect was observed. The beta phase( $\beta$ ) columnar grains were observed in the regions that exposed to temperature greater than 882 °C.

**D. Mpumlwana et al.**[16] proposed the mechanical characteristics of commercially pure grade 2 titanium plates after steady heat treatment at various heating periods. This study seeks to investigate the microstructure of CP-Ti grade 2 in relation to its mechanical properties. It was found that the effect of annealing time over the grain growth. The study also reported that the UTS of CP-Ti has reduced while percentage

elongation increases after increasing annealing time. Also, the decrease in micro-hardness with an increase in annealing time was reported. However, there is a sudden increase in the micro-hardness value with a higher annealing period.

**F. Javier Gil et al.**[19] investigated the effect of shot blasting on fatigue life and fracture properties of titanium. The study suggested that because of the increase in surface roughness during shot blasting the osseointegration of dental implants made out of CP-Ti has improved.

**K. Gurusami et al.**[20] investigated the effect of two mechanisms of the Laser shock peening (which are direct and confined) on the mechanical properties of casted CP-Ti. The study postulated that the pulsed ablation provides better surface roughness in comparison to the continuous ablation mode. Higher compressive residual stresses were obtained during confined ablation. The uniform microstructure and enhanced mechanical properties were achieved after LSP. On the contrary, during direct ablation mode, the microstructure enhancement was not uniform and a burning effect was observed on the surface layer.

**H. Attar et al.**[21] aimed to perform a comparative study on three different AM techniques by observing the microstructure, mechanical, and wear properties of CP-Ti produced by SLM, LENS, and WAAM techniques. The microstructure investigation revealed the smallest grains in SLM-built samples, while the grain size obtained from WAAM has the largest size. The WAAM fabricated part showed the maximum ductility of the three processes used. The elastic energy of the fabricated part from SLM is more than that produced by LENS and WAAM. The results obtained during this study inferred that the fabricated samples from SLM exhibit better wear resistance and strength.

**Hyung-Ki Park et al.**[22] studied the effect of cyclic heat treatment over EBAM fabricated part. The study aimed to reduce elastic modulus using

the cyclic heat treatment method without using any mechanical method to do the same. The study proposed that there is a significant decrease in the young's modulus, grain refinement, and anisotropic grain morphology changed over the fabricated part.

**L.J. Wu et al.**[23] investigated the combined influence of service temperature and large LSP on CP-Ti alloy tensile properties, tensile characteristics, and micro-hardness evolution were investigated by the author. High temperatures were found to be ineffective in improving micro-hardness., but LSP improves micro hardness significantly. It was also inferred that because of grain growth at increasing temperature reduces the UTS but LSP improves the UTS, area reduction of the fracture surface. LSP also improved plasticity.

**P.A Dearnley et al.**[24] investigated the comparison of corrosion-wear behavior of untreated and oxidized CP-Ti and Ti<sub>6</sub>-Al<sub>4</sub>-V in physiological saline and a rapid assessment for biocompatibility. It was concluded from the research that there is a significant increase in the hardness value by the formation of TiO<sub>2</sub>(Rutile) layer over the surface, and corrosion-wear resistance of CP-Ti and Ti<sub>6</sub>-Al<sub>4</sub>-V also improves with the formation of the oxide layer.

**Y. Sasikumar et al.**[25] attempted to study the surface modifications of CP-Ti and Ti<sub>5</sub>Al<sub>2</sub>Nb<sub>1</sub>Ta by using alkali, hydrogen peroxide, and heat treatment to study bioactivity. During the study, the authors came the conclusion that the surface-treated CP-Ti sample shows more bioactivity in comparison to the surface-treated Ti<sub>5</sub>Al<sub>2</sub>Nb<sub>1</sub>Ta.

**Furqan A. Shah et al.**[26] conducted a comparative study between CP-Ti and Ti<sub>6</sub>Al<sub>4</sub>V over the manufacturing process, bone tissue, and bacterial response. It was suggested that both CP-Ti and Ti<sub>6</sub>Al<sub>4</sub>V shows similar morphology, topography, and phase composition. The authors also inferred that both the machined material show a similar response to the osteointegration and biomechanical anchorage.

**Wen-Fu Ho et al.**[27] studied about the microstructure, tensile properties, and corrosion behavior of as cast Ti-7.5Mo and compared with that of CP-Ti, Ti-15Mo and Ti<sub>6</sub>Al<sub>4</sub>V alloys. It was found that CP-Ti and Ti-7.5Mo have similar corrosion resistance, which is higher than the above-mentioned materials.

**Young-Sin Choi et al.**[28] conducted a study regarding the fatigue limit, fracture mechanism, and mechanical property of the EBM fabricated part of CP-Ti and Ti<sub>6</sub>Al<sub>4</sub>V. The fabricated part from EBM shows higher mechanical properties like UTS, YS, elongation, and fatigue strength in comparison to conventional CP-Ti specimen. The samples fabricated at an optimum set of parameters using EBM showed similar mechanical properties to conventional Ti<sub>6</sub>Al<sub>4</sub>V. So, it was suggested to change the process parameters of EBM to get superior mechanical and fatigue strength.

**B.B. Zhang et al.**[29] studied the dissolution behavior, cytotoxicity, and film surface test for Ti-Ag alloys. After comparing the results of Ti-Ag alloys and CP-Ti, the authors concluded that Ti-Ag alloys show higher corrosion potentials, greater impedances, and lesser capacitances, all of which are indicative of nobler electrochemical activity. The cytotoxicity tests conducted reveal that the cell viability of Ti-Ag alloys is the same as CP-Ti.

**C.N. Elias et al.**[15] suggested that the excellent biocompatibility of CP-Ti is the result of the formation of the stable and inert oxide layer. The author also revealed various physical properties of CP-Ti, which makes it an excellent biocompatible material that includes low electrical conductivity, efficient corrosion resistance, the thermodynamic state is stable at physiological pH values, and ion production is low in aquatic conditions. Also, for the better anchorage of implant, ultra-fine grains are very beneficial.

**M. Vignesh et al.**[30] discussed various additive manufacturing Friction Stir Additive Manufacturing (FS-AM), laser additive manufacturing, selective laser melting (SLM), and Paste Extrusion Deposition (PED) are examples of such techniques. The authors surveyed the AM of Ti, Co, Mg-based implants in this article.

**Patrick H. Warnke et al.**[31] aimed to culture human osteoblast over SLM fabricated Ti<sub>6</sub>Al<sub>4</sub>V to check for biocompatibility. Furthermore, the occlusion of pores of various widths by osteoblast growth was assessed at various stages of the developed cell culture. The porosity and compressive strength of scaffolds with various pore diameters were also investigated. The Ti<sub>6</sub>Al<sub>4</sub>V scaffolds generated by SLM were shown to be biocompatible, allowing for total proliferation of all 0.5mm pores and a significant fraction of 0.5mm–0.6mm osteoblasts with a well-spread morphology.

**Ding K et al.**[10] showed the mechanisms involved in laser shock peening and reported that the depth of penetration in the case of LSP is more in comparison to shot blasting. LSP process helps in improving the fatigue life and surface properties. The author found that the fatigue life of the damaged part is equal to or even higher than the undamaged part after LSP. In comparison to shot peening, LSP is more beneficial in stress corrosion cracking resistance of thermally sensitized materials.

**Mohamed Abdel-Hady Gepreel et al.**[32] discussed the mechanical biocompatibility and emphasized the lower young's modulus for the choice of material during material selection for implant application. It was found that the  $\beta$ -type Ti alloys are most suitable for the formation of metallic implants.

**Ying Long Zhou et al.**[33] investigated the biocompatibility and corrosion resistance of Ti-Ta alloys and compared the result with CP-Ti. During experimentation, it was seen that significant doping of Ti with Ta

gives better corrosion resistance and biocompatibility to the alloy than pure titanium.

**Arash Ataee et al.**[34] conducted comparative study at the nano-level on the SLM manufactured CP-Ti and EBM manufactured Ti64 gyroid scaffolds. The SLM CP-Ti with porosity exhibited excellent biocompatibility and superior mechanical properties in comparison to EBM manufactured Ti64. Also, the mechanical properties in the scan direction gave superior value in comparison to the build direction.

### ***Literature Gap***

After going through available published literature, it is inferred that the AM of Titanium alloys has been performed using powder-based processes like SLM and EBM. The mechanical properties obtained using the afore-mentioned processes are promising and suitable for biomedical applications. The design freedom obtained using the powder-based processes is more than the wire-based process, but the processing time is significantly high. The wastage of the raw material is more in case of powder-based processing since after each micro level processing the unused powder is discarded. The printing time of fabrication from the powder-based process is much large than the Wire-based process. The interest has been gravitated toward the wire-based processing using arc as a heating source for faster and economical processing. [35] The surface modification of CP-Ti alloy has been attempted in various literature. Still, treatment on the WAAM fabricated CP-Ti has not been attempted to the best of my knowledge. Improvement in surface properties helps in increasing the biocompatibility of the fabricated product.

## Objectives

To fabricate defect-free CP-Ti alloy using the WAAM process for potential bio-medical application.

- To develop the wire-based AM system using arc-based welding technique.
- To develop the optimum compositions of CP-Ti alloys by using the WAAM system and optimization of process parameters.
- Systematically understand the evolution of deposition quality (cracks, porosity), microstructure, phase formation, and mechanical properties of deposited alloys.
- The effect of laser shock peening on the residual stress, surface morphology, microstructure, and phase transformation will be investigated.
- To investigate the biological properties of the structure prepared via WAAM and after surface modification via LSP.



## Chapter 3

# Experimental Program

### 3.1 Design of experiments

For the design of experiments, we explored two methods:

- **OVAT Analysis:** The ‘One Variable At a Time’ (OVAT) approach is formulated to optimize the process by keeping one parameter fixed and changing other parameters until all factors' effect is recorded and analyzed. However, this approach is very time-consuming.

To reduce the time input, Taguchi proposed a particularly developed method called orthogonal array to examine the complete parameter space with a minimum number of experiments.[36]

After considering this, the Taguchi approach is selected for the present study.

- **Selection of Taguchi Array:** The design of experiments using the orthogonal array is used. In most cases, this method is more efficient in comparison to other statistical designs.

$$N = \sum_{i=1}^{NV} (L_i - 1)$$

In the present study, there are two independent variables, i.e., voltage and feed rate of wire with three levels each.

Hence, minimum number of experiments to be performed are =  $1 + (3-1) + (3-1) + (3-1) = 7$ . Now, considering the Taguchi's orthogonal array: 3-Level Arrays: L9, L18, L27 Level So, an array closest to the number of experiments to be conducted is considered. Therefore, for this study, Taguchi's L9 orthogonal array is selected with three factors at three levels.

➤ **Selection of Levels of Process Parameters:**

Using OVAT Analysis, it is found that the threshold parameters as 16 volts and 5 m/min wire feed rate. Later, for the purpose of deposition, Taguchi's L9 orthogonal array is used for getting more accurate parameters for deposition as shown in Table3.1.

**Table3.1 Taguchi's L9 Orthogonal Array**

Sl.no	A	B	Sl.no	Voltage (V)	Wire feed (m/min)
1	1	1	1	16	5
2	1	2	2	16	5.8
3	1	3	3	16	6.5
4	2	1	4	16.5	5
5	2	2	5	16.5	5.8
6	2	3	6	16.5	6.5
7	3	1	7	17	5
8	3	2	8	17	5.8
9	3	3	9	17	6.5

### **3.2 WAAM of CP-Ti**

WAAM of CP-Ti during the experimentation was done using MIG-based (ESAB Inverter MIG-400 model) AM techniques. The setup in Figure 3.1 consists of a computer-based system via HELIX software is used for giving G-codes to the motor drivers to give the lead to the torch mounted on the CNC cradle in x, y, and z directions. The feedstock is supplied using a wire feeder, and XY stage moves the welding torch. During experimentation the deposition was done in only one direction to get a uniform micro structure and allowing cooling-off during deposition of successive layers. Scanning speed, argon gas flow rate, and standoff distance were all employed for deposition, and they were 8.57 mm/s, 20 L/min, and 15 mm, respectively. Above mentioned parameters are not varied and are kept fixed for the wall deposition.

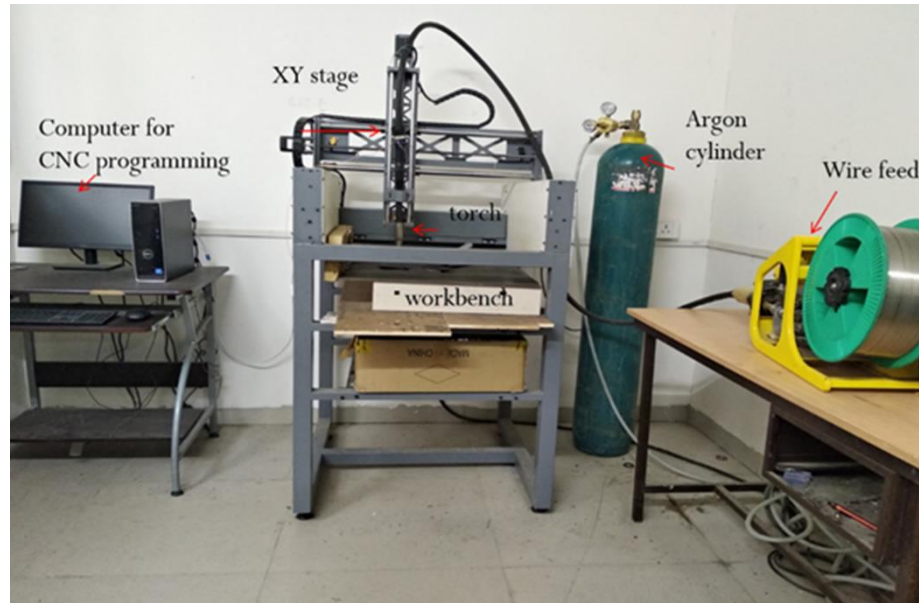


*Figure 3.1 Setup for Wire Arc Additive Manufacturing*

## **3.3 Metallographic Sample preparation and Characterization**

### **3.3.1 Wire EDM(W-EDM)**

The ECO-CUT wire EDM of consumables type was used to cut specimens using brass wire and DI water from wall structure with a resolution of 0.001mm and wire tolerance kept at 0.25mm to cut the work-piece from raw material.

### **3.3.2 Metallography Steps used for sample preparation**

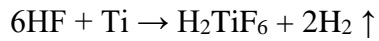
Standard metallography steps were used for the preparation of samples:

- Specimens are cut using W-EDM were polished on emery paper of grit size of 1000 to 2500.
- After that, samples were polished using a diamond paste of 0.5microns size over velvet cloth to get a finely polished surface.

Samples were checked for scratches over the Leica stereo microscope after final polishing.

### 3.3.3 Etching

Samples after polishing are chemically etched using Kroll's Reagent, which is 92 parts DI(De-Ionized) water, 6 parts HNO<sub>3</sub>(Nitric Acid), and 2 parts HF (Hydro Fluoric Acid) for 2 seconds. Swab etching is done using cotton and then rinsed under running water. The reaction of titanium and hydrofluoric acid is as shown[37]:



### 3.4 Heat Treatment

For heat treatment, samples are placed in quartz glass tubes. Two glass tubes are prepared as shown in Figure 3.2(a) using the glass blowing technique for keeping five samples in each tube. The quartz material is chosen so that we can have a heat resistance of glass above 900°C. The samples after being stored in the glass tube are sealed after removing air from the tube and creating a vacuum in the tube of magnitude  $1.9 \times 10^{-5}$  bar. The heat treatment using the quenching process is chosen for grain refinement and phase change. After sealing the glass tube, the samples are heat-treated in a muffle furnace as shown in Figure 3.2(b).

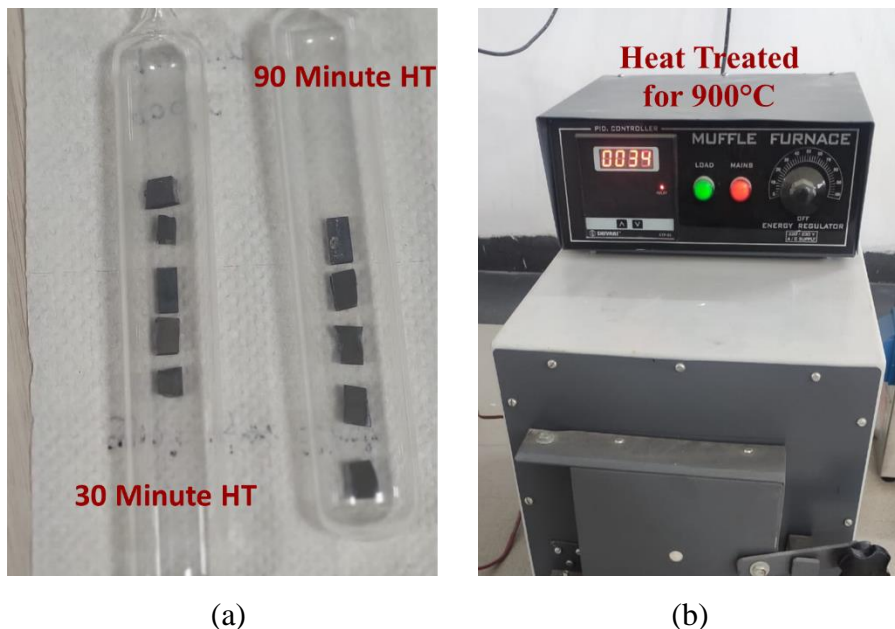


**Figure 3.2 Heat Treatment setup used (a) Vacuum Glass tube  
(b) Muffle Furnace**

The temperature of 900°C was first maintained in the furnace, and then the sealed glass tube with samples is placed inside the furnace and then is kept in the furnace at that temperature for 30 minutes and 90 minutes. After the above said time, the glass tubes are taken out from the furnace and are immediately placed inside a bucket of water, and the glass tubes are broken inside the water itself.

### **3.5 Laser Shock Peening**

In this work, laser shock peening of the CP-Ti by Q-switched mode Nd:YAG pulse laser source of the wavelength of 532 nm with 40% overlap to adjacent spot has been carried out. the setup used is as shown in Figure3.3. The parameters to be used for the process are set in such a way that the laser power comes out to be 0.5 joules with one pulse for every 10 ns for 532nm wavelength laser. Servo motor is used to move XY stage for even processing. The pulse density of the LSP process was measured by the speed of the translation stage. The beam diameter of the laser was controlled by altering the place among the sample and focusing lens of 200mm focal length. Experimental parameters as set during processing are as shown in Table3.2. A protective layer on the sample in the form of black insulation tape is used to shield the sample surface from the heating effect. Thus, only a mechanical effect is provided over the surface of the sample during the process. Water in the form of a medium is used to prevent plasma from escaping and prolong the effect of the shock generated. The medium is chosen in such a way so that it is not too viscous, which could absorb the shock generated and prevent it from getting transmitted to the sample surface. Therefore, the medium type and height of the medium should be considered accordingly. During the experimentation the medium(water) height is 5mm above the sample surface.

**Table 3.6 Experimental parameters**

Wavelength	Power	Focal Length	Pulse	Spot Dia.	Fluence
532 nm	0.5J	200mm	10ns	1.2mm	0.44J/mm <sup>2</sup>



**Figure 3.3 Laser Shock Peening Setup**

### **3.6 Microhardness testing**

Micro hardness testing employs indentation to probe the surface of a sample and measure the resulting impression. The properties of the specimen's microstructure in and around the depression are commonly determined using photographic equipment that improves the image of the indentation. The Vickers hardness number (HV) is the ratio of the force applied to the indenter (kgf) to the indentation's surface area (mm<sup>2</sup>).[38]

The formulae for the measurement of vicker's hardness value:

$$HV = \frac{2P \times \sin(\theta/2)}{D^2} \quad [\text{eq. 1}]$$

### **3.7 Biocompatibility Testing**

In this work, the biocompatibility testing performed on is antibacterial characteristics of CP-Ti. The samples prepared for testing are in the form of a disc having a diameter of 3mm and 2mm thickness. The bacteria

used for testing is *Staphylococcus Aureus*. The bacteria considered for testing is common bacteria which can attack at the tooth canal and knee cap surface.

During the experimentation Steps followed are as shown in Figure3.4. At very first, we grew the afore-mentioned bacteria in LB (Lysogeny Broth) medium for 36 hours. The time period for the incubation for the growth of bacteria depends on the doubling time of the bacteria under study. For *Staphylococcus Aureus* is around 24 minutes under typical laboratory conditions, which is kept in LB medium and incubating it at 37°C. After the growth of bacteria for 36 hours, the bacteria are taken out of the incubation chamber. They are centrifuged for 5000 rpm for 5 minutes so that bacteria get settled down at the bottom in the form of a pellet and get separated from the exhausted LB medium. After the separation of the bacteria in the form of pellet, again the pellet is centrifuged in fresh LB broth medium at same parameters so that dead bacteria can get separated.

Upon getting fresh live bacteria, the Observation density (OD) of the bacteria is checked so that we can get information regarding bacterial growth and the age of bacteria. Usually, the age of bacteria whose growth is at exponential level is considered for testing purposes. To check the OD initially, we reduce the concentration of the bacteria in the LB medium to bring the expected OD to the machine parameters. The ratio in which bacteria is mixed with fresh LB medium is 1:10, i.e., one-part bacteria and ten parts LB medium. After diluting the concentration of bacteria in the LB medium, we put the bacteria with LB medium inside a 96 well plate of 200 micro liter capacity. A pure LB medium without bacteria is also placed inside the well plate to get a standard value regarding the OD of broth. The well plate is then placed in a SYNERGY H1 microplate reader where the well plate is irradiated to a 600nm wavelength light wave and are checked for the OD of the standard i.e., broth and bacteria in LB medium. The observations given by the microplate reader are as shown in Table3.3.

**Table 7.3 Optical Density Measurement**

Sample	Observation1	Observation2	Observation3	Average
Broth	0.066	0.066	0.064	0.0653
LB medium with bacteria	0.143	0.144	0.145	0.144

The above mentioned average value of OD is of diluted medium. Hence, to get OD of the actual medium:

$$0.144 \times 10 = 1.44$$

To get the OD of bacteria, we need to remove the OD of broth from the overall OD of the bacteria in LB medium

$$1.44 - 0.0653 = 1.3747$$

Hence, the value 1.3747 is the actual OD of the bacteria.

After getting the value of the OD, we need to set the value of OD to 0.1  $\mu\text{l}$  and 1000  $\mu\text{l}$  for anti-bacterial testing. For setting of OD, we need to know the volume of Bacteria and LB medium to be taken out for testing, and for that, we use the following equation

$$N_1 V_1 = N_2 V_2 \quad [\text{eqn. 2}]$$

$$1.37 \times (x) = 0.1 \times 1000$$

$$(x) = 72.99 \mu\text{l} \approx 73 \mu\text{l}$$

Therefore, from the above equation, it is concluded that 73  $\mu\text{l}$  of LB-bacteria medium and 927  $\mu\text{l}$  of broth is used to prepare a final solution for anti-bacterial testing.

**06. Reincubation**

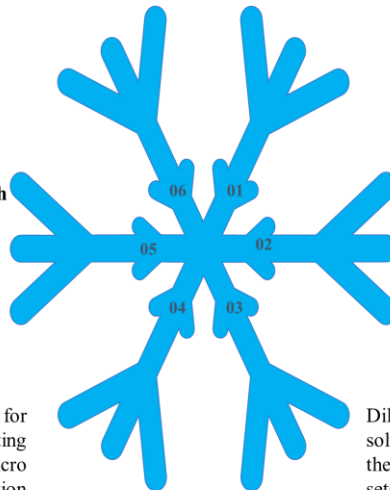
Petri dish is again put in the incubation chamber for the bacteria growth over the petridish.

**05. Preparing Petri dish**

Agar environment is maintained in petridish for action of bacteria over the samples prepared

**04. Setting up OD**

The OD is set at 0.1 for the preparation of Testing medium and 1000 micro liters of bacteria solution is prepared



**01. Incubation**

36 hours in LB Medium

**02. Centrifuging**

Done twice 1st to remove bacteria from incubation solution, 2nd to remove dead bacteria from live ones.

**03. Checkig OD**

Diluted bacteria in fresh LB solution in 1:10 ratio and then irradiating the sample sets in 600nm wavelength

**Figure 3.4 Steps utilized during Anti-Bacterial Testing**

During the final step of the experiment, a petri dish is prepared by putting broth over the dish and allowing it to spread evenly and solidify to form agar and later 100 µl of 0.1 OD bacteria. LB solution is spread evenly over the surface till dry and later samples prepared as mentioned above are placed over the dish as shown in the Figure3.5 below.

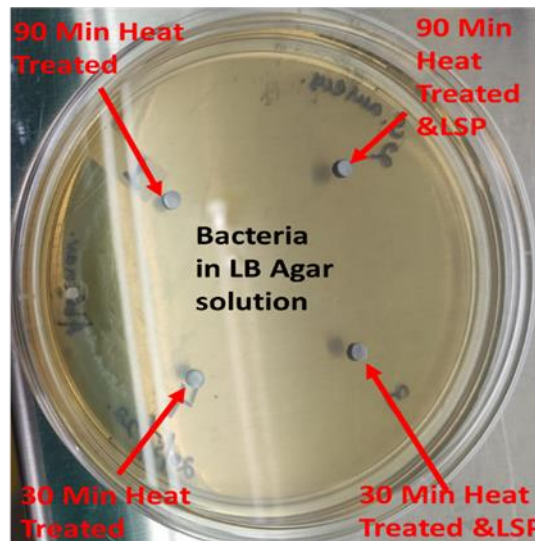


**Figure 3.5 Petri dish prepared for Anti-Bacterial Testing**



## Chapter 4

### Results & Discussion

#### 4.1 Process Parameter Optimization

The parameter optimization for the deposition of wire via WAAM is carried out to realise optimum process parameters for the bulk structure deposition i.e., voltage applied and wire feed rate. The optimization is reached in the following steps:

- Literature survey is done to get the threshold parameters for titanium alloy wire (NiTi) which is 17.3 V and 4.3 m/min wire feed rate[39]
- Since CP-Ti is also an alloy wire of titanium, it is considered that the threshold value at which deposition would occur would also come close to this value.
- Therefore, a Taguchi's L9 array is made from the above-mentioned values, and then the set of track deposition is done as shown in Figure 4.1.
- On observing the track deposited, the most continuous track with continuous height and width throughout the track is considered the most optimized parameter.



**Figure 4.1 Track deposition for parameter optimization**

After deposition of tracks, the tracks are cut using wire-EDM, and the after following all standard metallographic steps, the samples prepared

were observed under an optical microscope (Leica DMS 1000), and following observations were made-

1. Track deposited over mild steel substrate show very small weld pool formation, and the track did not stick properly over mild steel substrate. Therefore, a titanium substrate is used for further deposition.
2. The cracks are formed as shown in the Figure4.2. It could be caused due to hydrogen embrittlement.

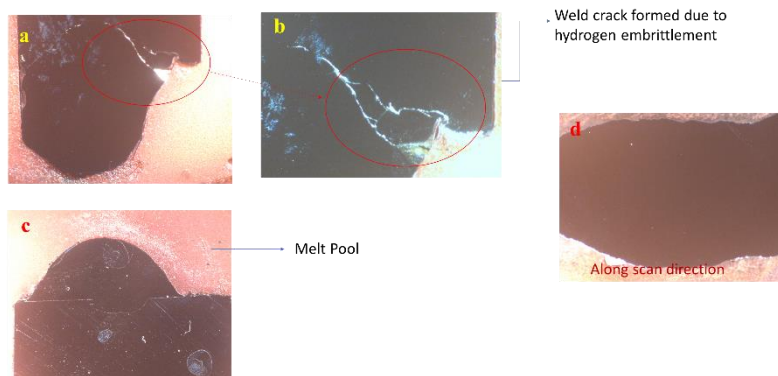


**Figure 4.2 Track Characterization**

## 4.2 Surface Porosity Measurement

Surface porosity measurement is done using the software feature of Dewinter's microscope for the measurement of surface porosity using image processing as shown in Figure 4.3.

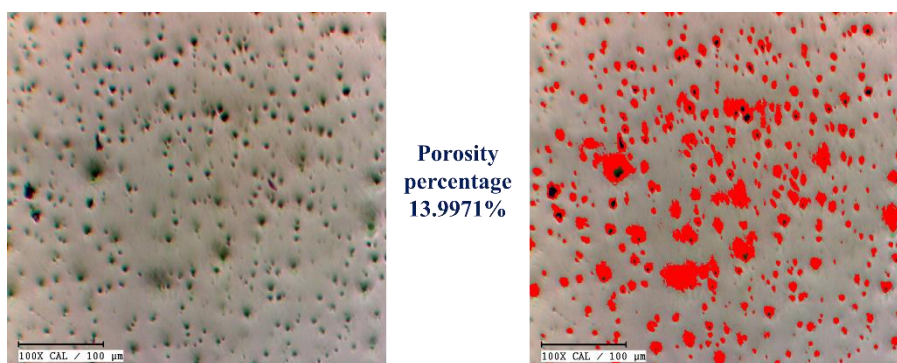


**Figure 4.3 Surface Porosity Measurement**

The image is first captured over the microscope, and then in the microscope software, we use the porosity option for the measurement of porosity. In the software, the image is processed, and a histogram of pixel density is formed based on the intensity of light, and the variation in the histogram gives the surface porosity percentage over the given surface.

### 4.3 Microstructure Study

Microscopic images were taken of the etched samples over Dewinter's microscope and observed for as-built samples as shown in Figure 4.4(a) below. The long columnar grains show the presence of  $\alpha$ -phase grains, and there were almost negligible any other phase present. The average grain size obtained is 11.8315  $\mu\text{m}$  in the columnar direction and 2.375  $\mu\text{m}$  in lateral direction. It can be concluded from the obtained optical images that after deposition of wire by WAAM there is only single phase deposition occurred. The mixed oriented grains are also obtained, but the shape of the grains remain columnar, as can be seen in Figure 4.4(b) The randomly oriented grains are obtained as the deposition has been done in both the direction i.e., in both +X and -X direction and the image captured at the interface.

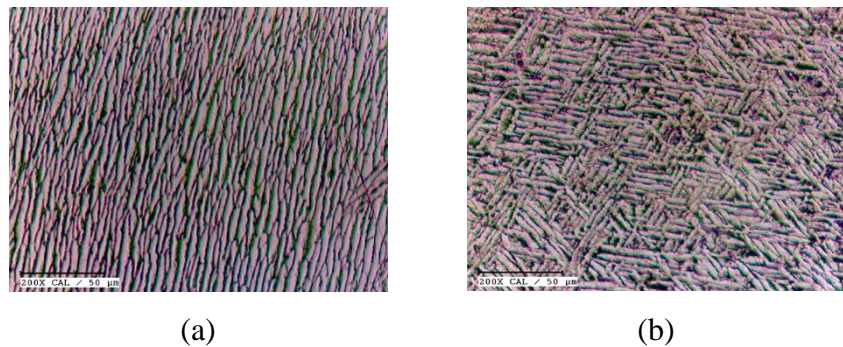


**Figure 4.4 Optical Image of CP-Ti as-built in deposition direction**

After heat treatment of the samples for 30 minutes and 90 minutes at 900°C, the samples are again etched and prepared to capture a microscopic image to check for the grain variation after heat treatment. The Figure4.5 below shows the formation of gobular shaped grains in both 30 minute heat treated sample Figure4.5(a) and 90 minute heat treated sample Figure4.5(b). The gobular grains represent the  $\beta$ -phase grains and columnar needle like grains show refined  $\alpha$ - phase grains after heat treatment.

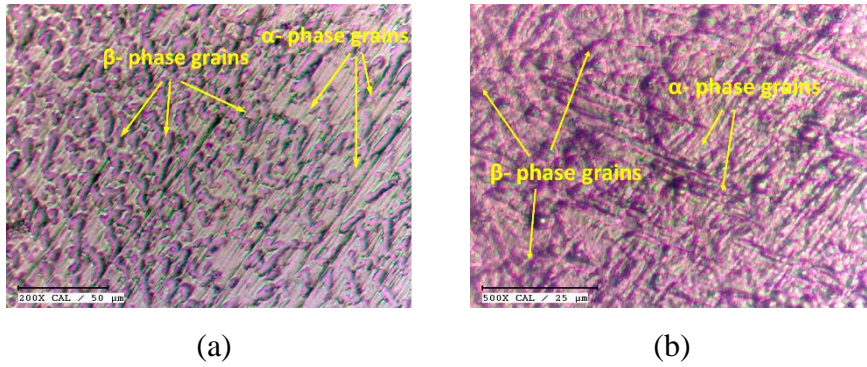


**Figure 4. 5 Optical Image of CP-Ti after Heat Treatment (a)for 30 minutes;(b) for 90 minutes**

In the current work, the samples after heat treatment have gone under laser surface treatment via Laser Shock Peening (LSP) process. The purpose of the mentioned process is to improve surface hardness and to increase surface roughness at the micron level. The said properties are varied by increasing the grain boundaries at the surface, by sudden heating and application of compressive stress simultaneously in turn increasing the number of grain boundaries at various orientation. The Figure 4.6 shows the optical image of the cross-section perpendicular to LSP treated surface. The average depth of the affected zone is 43.4476  $\mu\text{m}$  from Table 4.1

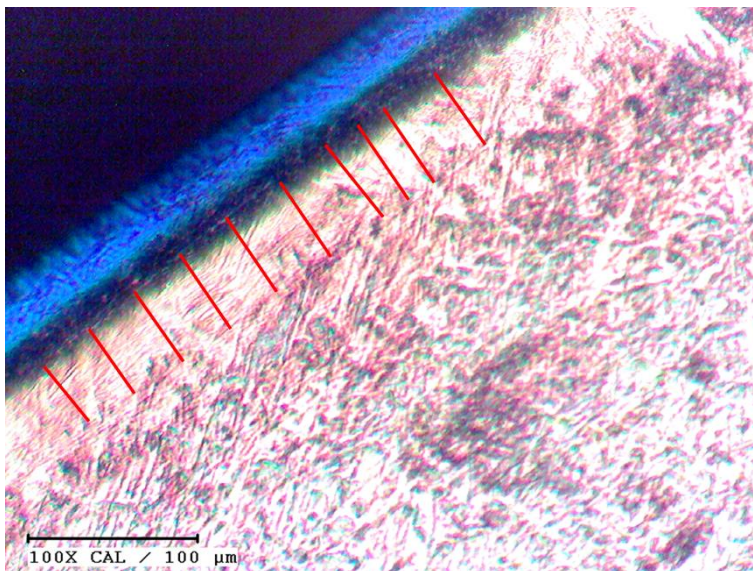


**Figure 4.6 Optical Image of CP-Ti after Heat Treatment (a)for 30 minutes;(b) for 90 minutes**

**Table 8.1 Length matrix to determine average affected depth after LSP**

Serial No.	Length ( $\mu\text{m}$ )
1	48.001
2	46.0005
3	46.3814
4	41.4587
5	38.3695
6	44.2286
7	43.6668
8	40.6923
9	43.2763
10	42.4009

## **4.4 Elemental Mapping Study**

When an electron beam collides with an atom's inner shell, one electron is knocked out of the shell, leaving a positively charged electron-hole. When an electron is displaced, an outer shell electron jumps in to fill the vacancy. As the electron goes from the higher-energy to lower-energy shell of the atom, the energy difference is discharged in the form of an X-ray. The X-rays created throughout the process are collected by a silicon drift detector, which is then analysed and interpreted by software. [40] The graph obtained during the elemental mapping is as shown in the Figure4.7(a). The Figure4.7(b) depicts the elemental mapping in the deposition direction, and there is no trace of any other material. Figure 4.7 shows traces of Carbon present, which signifies the diffusion of carbon into the wall structure during deposition from the mild steel substrate.

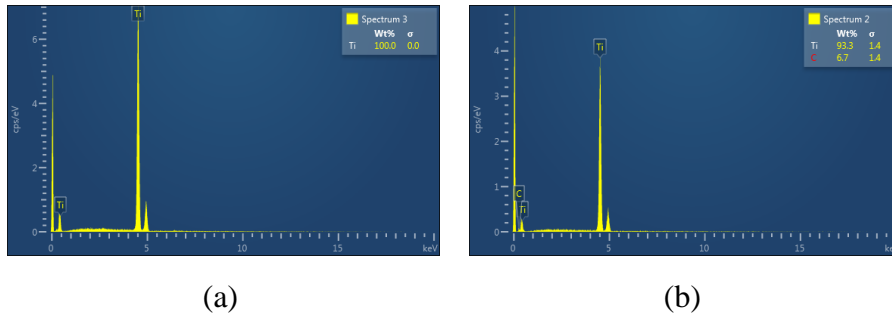


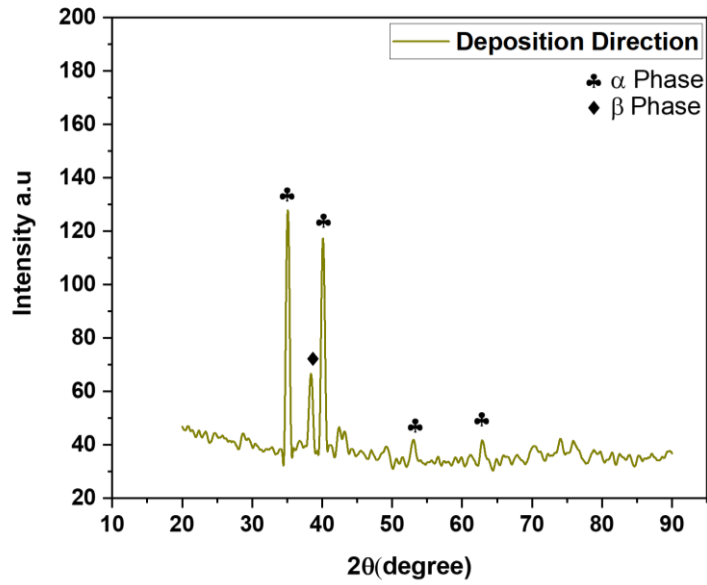
**Figure 4.7 EDX of CP-Ti along (a) Deposition Direction; (b) Build Direction**

## 4.5 Phase Analysis

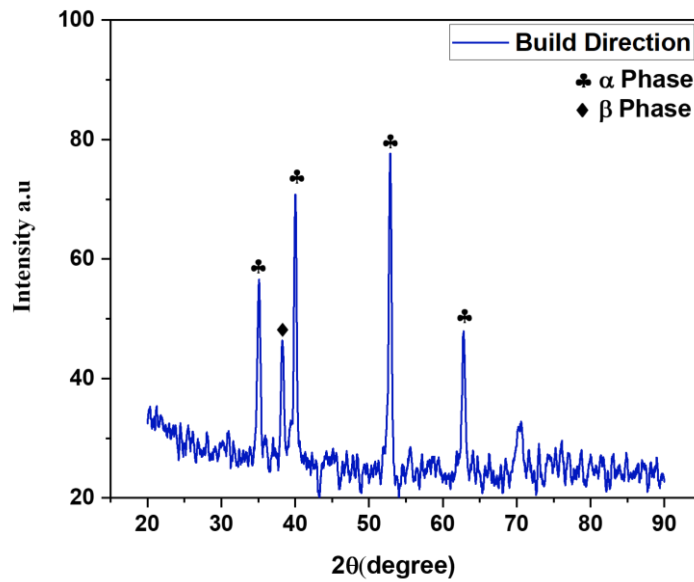
X-rays are electromagnetic energy waves, whereas crystals are atoms arranged in a regular pattern. A regular array of scatterers produces a regular array of spherical waves. Due to destructive interference, these waves cancel each other out in most directions, but they add constructively in a few select directions, as indicated by Bragg's law:

$$2d\sin\theta=n\lambda \quad [\text{eq. 3}] [41]$$

In this work, the XRD pattern obtained gave peaks in the range of  $20^\circ$  to  $100^\circ$   $2\theta$  value. The graph obtained after doing refinement and XRD analysis show the following peaks as shown in Figure 4.8. From the graph, it can be observed that there are a significant number of peaks of  $\alpha$ -phase and only single peaks for  $\beta$ -phase. Therefore, it can be concluded that the phase of the as deposited ample is  $\alpha$  dominant with almost negligible amount of  $\beta$  phase.



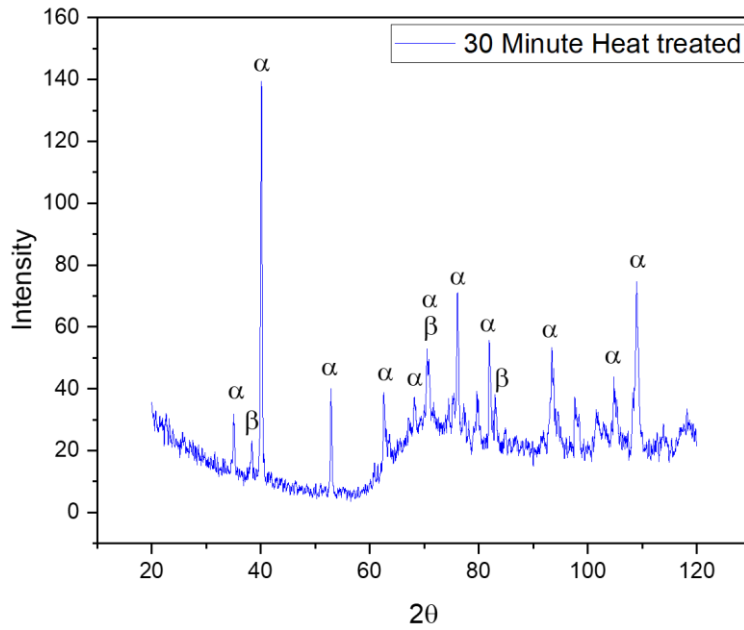
(a)



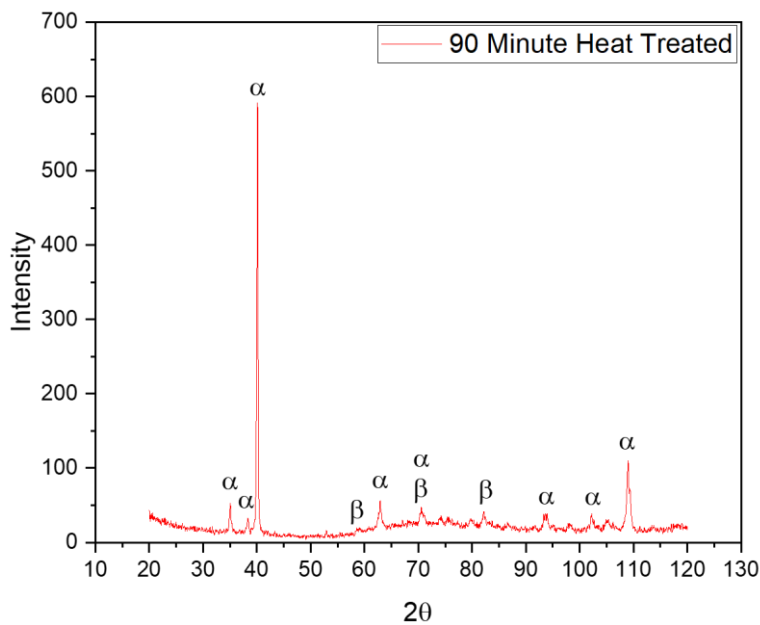
(b)

**Figure 4.8 XRD peaks of as-built CP-Ti along (a) Deposition Direction; (b) Build Direction**

In this study, the phase transformation is done to get the properties suitable for application purposes. It is seen that titanium undergoes an allotropic transformation at 882°C, below this temperature CP-Ti shows HCP crystal structure. And above 882°C temperature, it transforms into BCC crystal structure.



(a)



(b)

**Figure 4.9 XRD peaks of Heat Treated CP-Ti (a) for 30 minutes; (b) for 90 minutes**

## 4.6 Micro Hardness Analysis

Microhardness of the prepared samples is done over 5 samples of different categories which include samples in as-built condition, heat treated for 30 minutes, heat treated for 90 minutes. Also, samples heat treated for 30 minutes and for 90 minutes, respectively and followed by

LSP. The hardness value of the above-mentioned samples is as shown in the Figure 4.10. The Table4.2 shows the average value of micro-hardness of the above-mentioned samples.

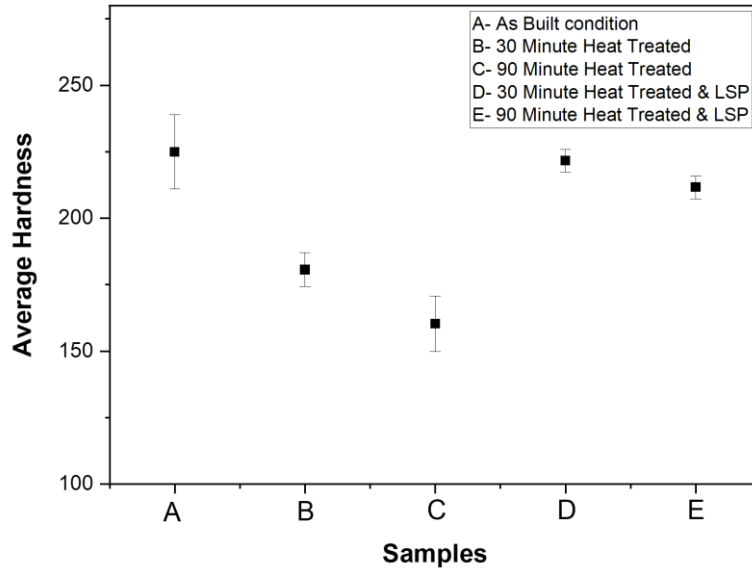


**Figure 4.10 Vicker’s Micro Hardness variation at different conditions**

**Table 4.2 Average Micro Hardness Values**

Sample Name	Average Vicker’s Hardness value
A	225
B	180.7
C	160.3
D	221.67
E	211.69

From the above table, the following can be concluded-

- The hardness value of the as-built sample is maximum.
- After heat treatment the hardness value decreases.
- Sample with longer heat treatment time period showed higher drop in micro-hardness value
- After LSP the micro-hardness improves.

## 4.7 Bio-compatibility Analysis

In this study, anti-bacterial testing is performed to check for the biocompatibility of the material. The inferences can be made after

observing the petri dish that is being incubated at 37°C in LB medium to facilitate the growth of bacteria. After incubating the petri dish for 12 hours, the condition of the petri dish is shown in Figure 4.11.

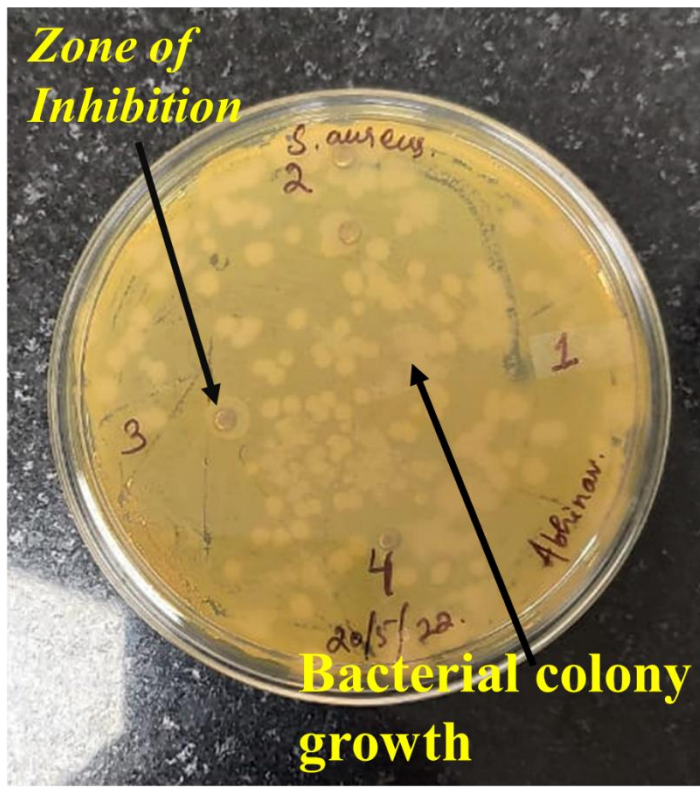


**Figure 4.11 Bacteria Colony Growth in Petri Dish**

The following observation was made after observing the petri dish. The Ring called *Zone of Inhibition* around the samples 2 and 3 signifies anti-bacterial characteristics of the specimen to the bacterial environment of *Staphylococcus Aureus*. This anti-bacterial phenomenon can be attributed to an increase in the number of grain boundaries owing to grain refinement and twinning after LSP, which facilitates the anti-bacterial effect. [42].

## Chapter 5

### Conclusions and Future Scope

#### 5.1 Conclusions

- ✓ **The optimum process parameters.**

Track deposition reveals that the most continuous track with even height and width comes at 16.5 V and 5 m/min feed rate of wire. It can be seen that at these parameters by keeping a stand-off distance of 15mm, scanning speed of 8.57 mm/sec, and argon gas flow rate of 20 L/min we get the optimized deposition. Therefore, these parameters are used throughout the experiments to do a further deposition of the wall structure.

- ✓ **The wall structure deposited has desired surface porosity of 13.9 %.**

The wall structure at the optimized parameter is deposited with ten layers to initial characterization. The deposition of wall was done in both to and fro-direction, so the wall structure obtained is thicker. To do further characterization, deposition is done only in one direction and the wall structure thus obtained has lesser width.

- ✓ **Microstructure studies revealed coarse columnar grain structure with  $\alpha$ -phase and  $\beta$ -phase.**

During initial characterization of the as-built structure revealed that only the  $\alpha$ -phase is dominant, and the significance of  $\beta$ -phase grains is negligible. The columnar grains obtained are coarse and have a size of 11.8315 $\mu$ m.

- ✓ **The XRD studies confirmed that the  $\alpha$ -phase is more dominant over the  $\beta$ -phase in as-built CP-Ti.**

The XRD data analysis reveals that for as-built sample, most of the peaks revealed  $\alpha$ -phase peaks, and only one of the peaks

represented  $\beta$ -phase peaks. Still, after heat treatment, there is a significant increase in the number of  $\beta$ -phase peaks and also  $\alpha$  &  $\beta$  peaks were observed.

- ✓ **It was evident from micro-hardness test that the surface hardness has reduced after heat treatment and has increased after Laser shock peening.**

The reason for the decrease in surface hardness can be attributed to the phase transformation of the grain and the change of HCP crystal structure to BCC type. The increase in the surface hardness after LSP is attributed to the increase in grain boundary density and accumulation of dislocation to the surface.

- ✓ **It was evident from the observation that the LSP treated sample showed a little amount of antibacterial effect.**

This is the result of the accumulation of grain boundaries and defects over the surface due to LSP, which affect the antibacterial nature of the material.

## 5.2 Future Scope

- ❑ **Extensive Bio-compatibility study**

The bio-compatibility study like cytotoxicity tests, sensitization assays, implantation tests, osteointegration can be performed to have a better understanding of the biocompatibility of CP-Ti

- ❑ **Cell viability test v/s surface morphology**

The effect of tissue connectivity to the surface and its variable surface morphology can also be studied. The surface roughness and its morphology play a vital role in the connection of tissue to the surface of the implant.

- ❑ **Other Surface modification techniques**

Surface modification techniques available are in abundance and each individual surface modification technique has its own pros. In current work, only mechanical modification technique is studied; other mechanical techniques, like PVD (Physical Vapour Deposition), should be explored as it improves wear resistance, corrosion resistance, and blood compatibility. Various other modification techniques like CVD (Chemical Vapour Deposition) and biochemical methods are also available to enhance the biocompatibility of biomedical alloys.[43]



## References

- [1] Ching, N. T., Ghobakhloo, M., Iranmanesh, M., Maroufkhani, P., & Asadi, S. (2021). Industry 4.0 applications for sustainable manufacturing: A systematic literature review and a roadmap to sustainable development. *Journal of Cleaner Production*, 130133.
- [2] <https://www.ge.com/additive/additive-manufacturing>. Accessed 20 May 2022.
- [3] Bourell DL, Frazier WE, Kuhn HA, M. Seifi, (2020), ASM Handbook: Additive manufacturing processes. ASM International 2020; 24:388-411.
- [4] Directed Energy Deposition ( DED ) What is Directed Energy Deposition ? How does Directed energy deposition work ? pp. 1–8. <https://engineeringproductdesign.com/knowledge-base/direct-energy-deposition/>. Accessed 20 May 2022.
- [5] Direct Energy Deposition | Laser vs. Arc vs. Electron Beam DED. pp. 3–6. <https://ewi.org/capabilities/additive-manufacturing/what-is-direct-energy-deposition/>. Accessed 20 May 2022.
- [6] MIG Welding : Principle, Working, MIG Welding : Principle, Equipment, Power Source, (2017), pp. 1–9. <https://www.mech4study.com/2017/04/mig-welding-principle-working-equipment-applications-advantages-and-disadvantages.html> 2/9. Accessed 20 May 2022.
- [7] K. M. Corporation, “the 3 Stages of Heat Treatment,” pp. 1–7, 2020, . Available: <https://www.kloecknermetals.com/blog/the-three-stages-of-heat-treatment/>. Accessed 20 May 2022
- [8] T. . Rajan, C. . Sharma, and A. Sharma, (2011) *Heat Treatment: Principles and Techniques, 2nd Edition*. PHI learning Private limited
- [9] T. S. N. Sankara Narayanan, I. S. Park, and M. H. Lee,(2015),

*Surface modification of magnesium and its alloys for biomedical applications: Opportunities and challenges*, vol. 1, no. . .  
<http://dx.doi.org/10.1016/B978-1-78242-077-4.00002-4>

- [10] K. Ding and L. Ye, (2006) “Physical and mechanical mechanisms of laser shock peening,” *Laser Shock Peen.*, pp. 7–46, , doi: 10.1533/9781845691097.7.
- [11] M. M. Miroshnikov and I. Nabiev, (1996) “Applications in Medicine,” *Raman Microsc. Dev. Appl.*, pp. 379–419,.
- [12] P. Biolabs, “LEARNING CENTER INTRODUCTION TO BIOCOMPATIBILITY WHAT IS DEVICE REQUIREMENTS FOR The best starting point for understanding biocompatibility requirements is.” <https://pacificbiolabs.com/biocompatibility-testing>. Accessed 20 May 2022
- [13] J. Black, “The education of the biomaterialist: Report of a survey, (1980–81),” *J. Biomed. Mater. Res.*, vol. 16, no. 2, pp. 159–167, 1982, doi: 10.1002/jbm.820160208.
- [14] G. M. Raghavendra, K. Varaprasad, and T. Jayaramudu, (2015) “Biomaterials: Design, Development and Biomedical Applications,” *Nanotechnol. Appl. Tissue Eng.*, no. January, pp. 21–44, 2015, doi: 10.1016/B978-0-323-32889-0.00002-9.
- [15] C. N. Elias, J. H. C. Lima, R. Valiev, and M. A. Meyers, (2008) “Biomedical applications of titanium and its alloys,” *Jom*, vol. 60, no. 3, pp. 46–49, , doi: 10.1007/s11837-008-0031-1.
- [16] D. Mpumlwana, V. Msomi, and C. J. S. Fourie,( 2021) “Effect of Heat Treatment on the Mechanical Properties of a 3 mm Commercially Pure Titanium Plate (CP-Ti Grade 2),” *J. Eng. (United Kingdom)*, vol., doi: 10.1155/2021/6646588.
- [17] S. Kara, (2012)*A ROADMAP OF BIOMEDICAL ENGINEERS AND MILESTONES.*
- [18] B. Wysocki *et al.*, (2017) “Microstructure and mechanical

- properties investigation of CP titanium processed by selective laser melting (SLM),” *J. Mater. Process. Technol.*, vol. 241, pp. 13–23, , doi: 10.1016/j.jmatprotec.2016.10.022.
- [19] F. Javier Gil, J. A. Planell, A. Padrós, and C. Aparicio,( 2007) “The effect of shot blasting and heat treatment on the fatigue behavior of titanium for dental implant applications,” *Dent. Mater.*, vol. 23, no. 4, pp. 486–491, , doi: 10.1016/j.dental.2006.03.003.
- [20] K. Gurusami, D. Chandramohan, S. Dinesh Kumar, M. Dhanashekar, and T. Sathish, (2020) “Strengthening mechanism of Nd: Yag laser shock peening for commercially pure titanium (CP-Ti) on surface integrity and residual stresses,” *Mater. Today Proc.*, vol. 21, no. xxxx, pp. 981–987, , doi: 10.1016/j.matpr.2019.09.141.
- [21] D. K. M. S. D. H. Attar, M.J. Bermingham, S. Ehtemam-Haghighi, A. Dehghan-Manshadi,(2019) “Evaluation of the mechanical and wear properties of titanium produced by three different additive manufacturing methods for biomedical application.” doi: <https://doi.org/10.1016/j.msea.2019.06.024>.
- [22] B.-S. L. H. G. K. . Hyung-Ki Park, Tae-Wook Na, Jong Min Park, Yanghoo Kim, Gun-Hee Kim,( 2019) “Effect of cyclic heat treatment on commercially pure titanium part fabricated by electron beam additive manufacturing,” doi: <https://doi.org/10.1016/j.jallcom.2019.04.335>.
- [23] L. J. Wu, K. Y. Luo, Y. Liu, C. Y. Cui, W. Xue, and J. Z. Lu, (2018)*Effects of laser shock peening on the micro-hardness, tensile properties, and fracture morphologies of CP-Ti alloy at different temperatures*, vol. 431.
- [24] H. Ç. P.A. Dearnley, K.L. Dahm,(2003)“The corrosion-wear behaviour of thermally oxidised CP-Ti and Ti-6Al-4V.” doi: 10.1016/S0043-1648(03)00557-X.

- [25] Y. Sasikumar and N. Rajendran, (2012) “Surface modification and in vitro characterization of Cp-Ti and Ti-5Al-2Nb-1Ta alloy in simulated body fluid,” *J. Mater. Eng. Perform.*, vol. 21, no. 10, pp. 2177–2187, , doi: 10.1007/s11665-012-0143-1.
- [26] F. A. Shah, M. Trobos, P. Thomsen, and A. Palmquist,(2016) “Commercially pure titanium (cp-Ti) versus titanium alloy (Ti6Al4V) materials as bone anchored implants - Is one truly better than the other?,” *Mater. Sci. Eng. C*, vol. 62, pp. 960–966, 2016, doi: 10.1016/j.msec.2016.01.032.
- [27] W. F. Ho, (2008) “A comparison of tensile properties and corrosion behavior of cast Ti-7.5Mo with c.p. Ti, Ti-15Mo and Ti-6Al-4V alloys,” *J. Alloys Compd.*, vol. 464, no. 1–2, pp. 580–583, , doi: 10.1016/j.jallcom.2007.10.054.
- [28] D.-G. L. Young-Sin Choi, Chang-Lim Kim, Gun-Hee Kim, Byoung-Soo Lee, Chang-Woo Lee, (2017)“Mechanical Properties Including Fatigue of CP Ti and Ti-6Al-4V Alloys Fabricated by EBM Additive Manufacturing Method.” .
- [29] B. B. Zhang, K. J. Qiu, B. L. Wang, L. Li, and Y. F. Zheng, (2012) “Surface Characterization and Cell Response of Binary Ti-Ag Alloys with CP Ti as Material Control,” *J. Mater. Sci. Technol.*, vol. 28, no. 9, pp. 779–784, , doi: 10.1016/S1005-0302(12)60130-3.
- [30] M. S. M. Vignesh, G. Ranjith Kumar and and N. A. M. Manikandan, G. Rajyalakshmi, R. Ramanujam,(2021) “Development of Biomedical Implants through Additive Manufacturing: A Review.” .
- [31] P. H. Warnke *et al.*, (2009) “Rapid prototyping: Porous titanium alloy scaffolds produced by selective laser melting for bone tissue engineering,” *Tissue Eng. - Part C Methods*, vol. 15, no. 2, pp. 115–124, , doi: 10.1089/ten.tec.2008.0288.
- [32] M. A. Gepreel and M. Niinomi, (2013) “Biocompatibility of Ti-

- alloys for long-term implantation,” vol. 20, pp. 407–415,.
- [33] Y. L. Zhou, M. Niinomi, T. Akahori, H. Fukui, and H. Toda, (2005) “Corrosion resistance and biocompatibility of Ti-Ta alloys for biomedical applications,” *Mater. Sci. Eng. A*, vol. 398, no. 1–2, pp. 28–36, doi: 10.1016/j.msea.2005.03.032.
- [34] A. Ataei, Y. Li, and C. Wen, (2019) “A comparative study on the nanoindentation behavior, wear resistance and in vitro biocompatibility of SLM manufactured CP–Ti and EBM manufactured Ti64 gyroid scaffolds,” *Acta Biomater.*, vol. 97, no. xxxx, pp. 587–596, , doi: 10.1016/j.actbio.2019.08.008.
- [35] Srinivas, M., & Babu, B. S. (2017). A critical review on recent research methodologies in additive manufacturing. *Materials Today: Proceedings*, 4(8), 9049-9059.
- [36] P. S. Deshmukh,( 2020) ““ Parametric Investigations of Laser Polishing ( LP ) of Laser Additive Manufactured ( LAM ) Structures of Hastelloy-X ’ Department of Mechanical Engineering Government College of Engineering , Aurangabad,”.
- [37] K. Y. Hung, Y. C. Lin, and H. P. Feng, (2017) “The effects of acid etching on the nanomorphological surface characteristics and activation energy of titanium medical materials,” *Materials (Basel)*,. vol. 10, no. 10, , doi: 10.3390/ma10101164.
- [38] CCSi, “Rockwell MicroHardness CCSi TechNotes : Basics of Rockwell MicroHardness Testing.” <https://www.ccsi-inc.com/articles/>.Accessed 20 May 2022
- [39] I. Ponikarova *et al.*,( 2021) “The effect of substrate and arc voltage on the structure and functional behaviour of NiTi shape memory alloy produced by wire arc additive manufacturing,” *J. Manuf. Process.*, vol. 70, pp. 132–139, , doi: 10.1016/j.jmapro.2021.08.026.
- [40] A. Nanakoudis, (2019) “EDX Analysis with SEM: How Does it

- Work?,” *Thermo Fish. Sci.*, pp. 2019–2022,.  
<https://www.thermofisher.com/us/en/home/materials-science/eds-technology.htm>. Accessed 20 May 2022
- [41] TWI, “What Is X-Ray Diffraction Analysis (Xrd) and How Does It Work?,” *Twi*, 2020. <https://www.twi-global.com/technical-knowledge/faqs/x-ray-diffraction>. Accessed 20 May 2022
- [42] I. S. Okeke *et al.*, (2021)“Impact of particle size and surface defects on antibacterial and photocatalytic activities of undoped and Mg-doped ZnO nanoparticles, biosynthesized using one-step simple process,” *Vacuum*, vol. 187, no. January, , doi: 10.1016/j.vacuum.2021.110110.
- [43] S. Izman *et al.*( 2012), “Surface Modification Techniques for Biomedical Grade of Titanium Alloys: Oxidation, Carburization and Ion Implantation Processes,” *Titan. Alloy. - Towar. Achiev. Enhanc. Prop. Divers. Appl.*, , doi: 10.5772/36318.